Most mineral assemblages do not show any effect of low temperature retrogression during this second folding stage. Moreover, these E-W fold structures show close relationships with most pegmatite dykes, especially with the two largest E-W dykes in the area (Fig. 50), since they are located in the hinge zone of a D_{2-3} hectometric fold. These relationships between folds and pegmatite dykes are very similar to some observed in the Culip-Cap de Creus area. For these reasons, the post-D_2 E-W folds in the Canal Guillosa area and vicinity have been correlated with the E-W structures in the Culip-Cap de Creus area, corresponding to the latest stages of high temperature progressive deformation. The name D_{2-3} folding stage results from this attempt of correlation.

Microstructures

The folding of the earlier S_2 foliation produces a new foliation, which appears at the microscopical scale as a typical differentiated crenulation cleavage, with reorientation of micas. Quartz and feldspar concentrate in the fold hinges, developing into microlithons. The medium-high grade mineral assemblages present in the rocks affected by D_{2-3} deformation are stable, without visible signs of neither low temperature retrogression, nor grain size reduction (Fig. 52). Moreover, some coarse micaschists show micas that grew at least partially after crenulation.

From these observations it is deduced that D_{2-3} structures formed around the time when peak metamorphism was reached, and continued under high temperature retrogressive conditions.

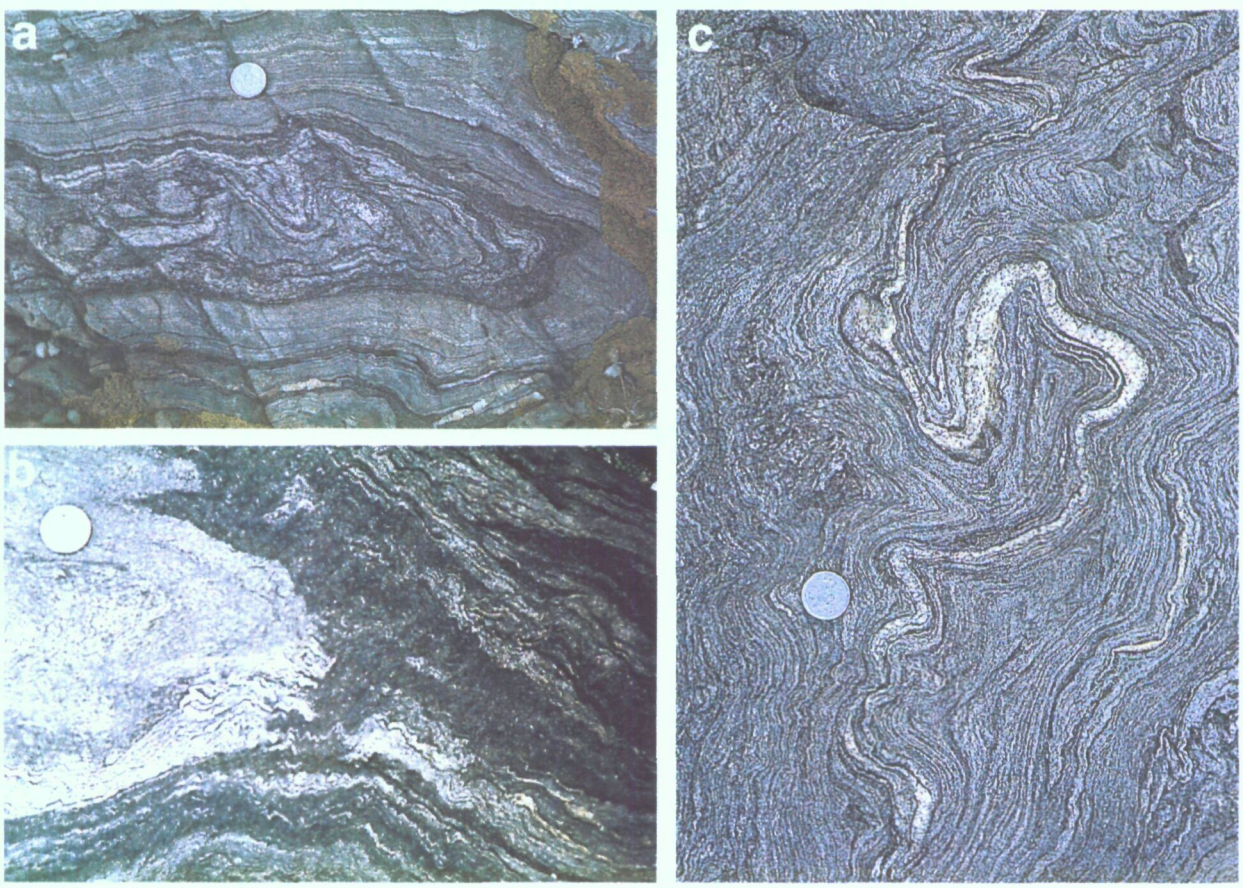

Fig. 51. Field photographs of interference structures (D_2 and D_{2-3} deformation). (a): Type 3 fold interference pattern, Cala Galladera. (b): F_2 folds transected by S_{2-3} crenulation cleavage, preferentially developed in the pelitic metasediments, Canal Guillosa. (c): Mushroom-like fold interference pattern affecting S_S/S_1 foliation and an early quartz vein, south Es Xiulet (photograph by Sebastià Gonzalo).

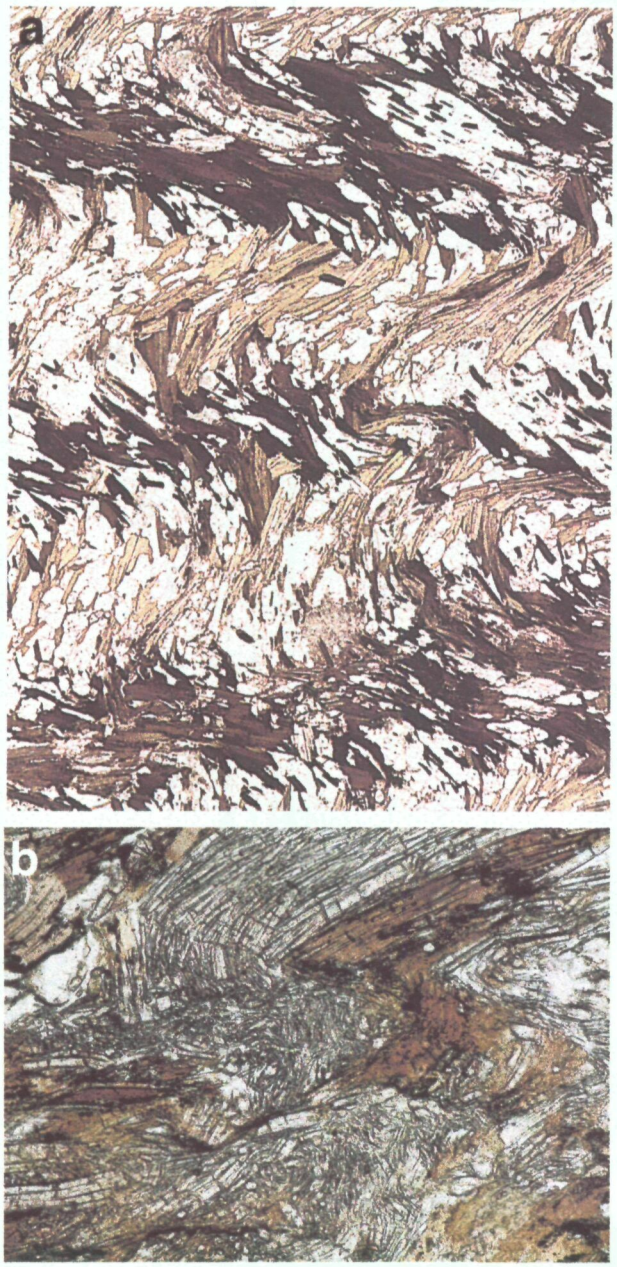

Fig. 52. Microphotographs of D_{2-3} structures. PPL. (a): Microfolds and incipient tectonic banding, high grade micaschist from Cala de sa Caixa. Width of view 7 mm. (b): Prismatic sillimanites folded by D2-3. Width of view 13 mm.

THE CALA BONA EXAMPLE

Another hectometric E-W trending fold is encountered in the Cala Bona area (Fig. 53). As in the Canal Guillosa example, the fold overprints bedding-S_1 and S_2 foliations, but differs from the former example in the dominant foliation, which is the S_1 schistosity at Cala Bona.

This zone consists of medium grade metasediments from the cordierite-andalusite zone, with some thin layers of quartzite (Culip and Rabassers types) and slices of rocks of the Sant Baldiri Complex. Both lithologies are in general sub-parallel to the bedding-S_1 schistosity.

D_2 deformational features are well displayed as fine crenulation cleavages developed in the metapelites and few minor "S"-shaped open folds, typical of D_2 low strain domains.

In the map (Fig. 53), small stereoplots correspond to three sub-areas that I have established. The sub-areas are relatively homogeneous in regard to D_2 deformation, as they are of similar low strain (i.e. similar angular relationships between the S_1 enveloping surface and S_2), but differ in the absolute orientations of S_1 and S_2. Thus, post-F_2 folding or shearing is necessary to explain the deformation of both surfaces. Superposed folds are scarce in this area, because of D_2 low strain.

Folds and axial planar crenulations affecting S_1 and S_2 foliations have variable attitudes, with E-W to NW-SE trends, and with moderate to steep northward dips. However, the spatial distribution of differently oriented post-D_2 folds seems to produce a vague structural zonation. In this way, the central structure is an approximately E-W fold, which increases in tightness towards the eastern seashores of Cala Bona. Going away from this main fold structure, axial traces of minor folds are closer to NW-SE orientations as approximating to late shear zones with also mainly NW-SE trends.

In this case, the E-W trending folds are difficult to distinguish from the NW-SE folds, both in style and metamorphic conditions. It seems that E-W folds and crenulations postdated the peak of metamorphism, and evolved into NW-SE F_3 late folds and shear zones at clearly retrograde conditions.

In this example and in other domains affected by low and medium grade metamorphism, E-W trending folds are intimately related to the late retrograde D_3 folding event, and have been labelled D_{2-3} folds. They correlate in general orientation and in relative age with D_{2-3} folds exposed in higher grade metamorphic zones.

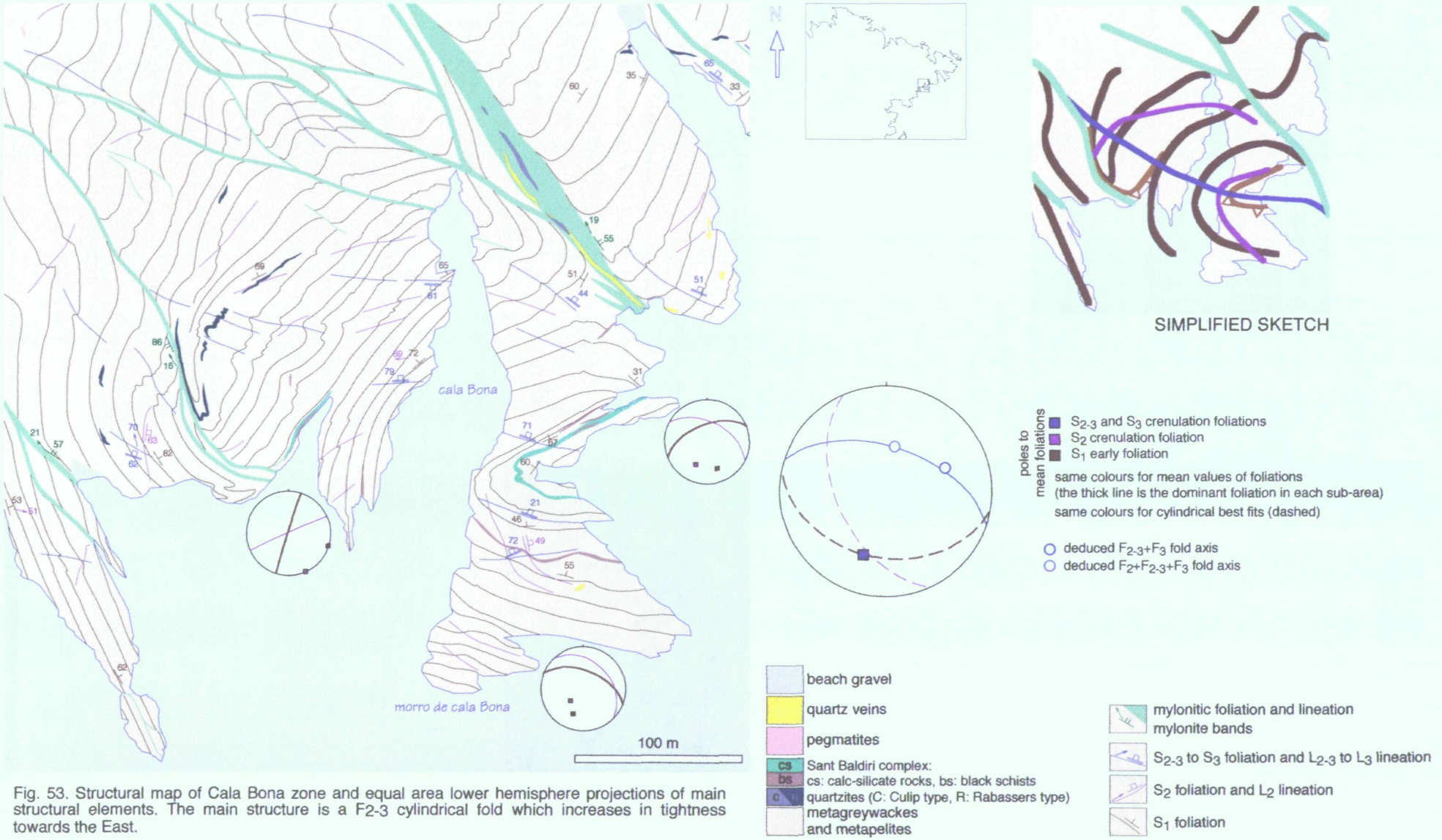

Fig. 53. Structural map of Cala Bona zone and equal area lower hemisphere projections of main structural elements. The main structure is a F2-3 cylindrical fold which increases in tightness towards the East.

4.5. LATE STRUCTURES: D_3 FOLDS AND SHEAR ZONES

These structures include folds and shear zones affecting the previous developed penetrative S_1 or S_2 foliations. Since the early works (Carreras 1975), late folds and shear zones have been regarded as contemporaneous structures arisen as the result of changes in the behaviour of schists and related rocks displaying a northwards increasing crystallinity, being deformed in low grade metamorphic conditions. Such interpretation was later extended to adjoining areas in the eastern Pyrenees (Carreras et al 1980), and developed in more detail for the Roses granodiorite (Carreras & Losantos 1982) and for the NE Cap de Creus peninsula (Carreras & Casas 1987). The intimate association of late folds and shear zones in the study area indicates that the above interpretation is essentially correct, and thus both structures, shear zones and folds will be examined concurrently and briefly.

As stated above, the prograde regional metamorphic zonation, developed before D_3, caused marked changes in rock properties at the time of D_3 deformation. While during D_2 rocks were deformed in different temperature conditions, at the time of the D_3 deformational event, retrograde conditions were rather homogeneous. On the contrary, a marked change in crystallinity of the deforming rocks was very significant. In such setting, rocks which had not exceeded low grade were deformed mainly by folding, while medium to high grade schists accommodated deformation essentially by shear zone development. In such situation, a second structural zoning arose, with a fold belt, covering the southern part of the studied area and the central and southern part of the whole Cap de Creus peninsula, and a mylonite belt, tracking the higher grade metamorphic zones and also present in the granodiorites of Roses and Rodes. A complex transition zone with coexistence of folds and shear zones has been recognized. Although detailed structural analyse reveal the existence of occasional shear zones in the fold belt and late folds in the mylonite belt, the prevalence of the specific structure in each domains validates the zonation (Fig. 54).

4.5.1. LATE FOLDS

D_3 folds are specially developed in low grade zones and thus they affect predominantly S_1, the planar fabric controlling folding. Folds in the transition zone can affect either S_1 or S_2 as the prevalent folded foliation, depending on domains. These folds range from major to minor, are SW-verging, and have NW -SE trending axial planes with NE gently to moderate dips. While the orientation of the axial planes is rather homogeneous, the fold axes show a gradual change in orientation. While moderate plunges predominate in the southern part of the studied area, to the northeast, these fold axes have gradually steeper attitudes and north directions (Fig. 37). The absence of later folds affecting their axial planes suggests that this dispersion is an original attitude, associated to the pre-D_2 macrostructure (section 4.2).

Carreras & Casas (1987) examined the geometry and orientation of these folds in the transition zones, and showed the existence of two main determinants in their geometry. On one hand, the attitude of the previous foliation controls the development of "S", "Z" or "M" folds, and thus asymmetries do not respond exclusively to the position with regard to the contemporaneous major folds, but to the previous structures. In addition, the attitude of the axial planes and fold axes depends on strain intensity, with axial planes and stretching lineations rotating respectively towards the NW-SE and to the NNW with increasing strain. These directions correspond to the main trend of the shear zones and of the associated stretching lineation.

A significant difference between the here exposed structural development and previous descriptions (e.g. in Carreras & Casas, op. cit.) concerns the E-W trending folds. These folds are here ascribed to the D_{2-3} stage while the authors considered them as initial stages of late folds. While it is accepted that the folds could develop in early stages of the late event, the manifest different thermal conditions existing in the north-seated domains at the time of E-W folding and NW-SE shearing leads to separate these structures. However, it is not excluded that the E-W folds represent early stages of a progressive deformation, while the NW-SE folds represent the latest stages of this event. This is specially manifest in lower grade domains where, in

addition, there is no significant change in metamorphic conditions during these events.

D_3 folds also exhibit a marked heterogeneous distribution across the area, enabling to distinguish zones of lower and higher D_3 strain (Fig. 55), in a similar way than in the D_2 event. In this case, domains of high strain are represented by relative narrow NW-SE trending bands of intense folding and transposition (and associated mylonitization, Fig. 55b). Northwards, many of these transposition bands connect with the typical shear zones (Fig. 54).

The heterogeneous distribution of both D_2 and D_3 structures give rise to a variety of structural relationships. However, F_3 folding was mostly developed over low grade domains with a pervasive S_1 foliation (i.e. low D_2 strain domains) and, therefore, the most common features are those resulting of overprinting of the S_1 schistosity by D_3 structures (Fig. 55a).

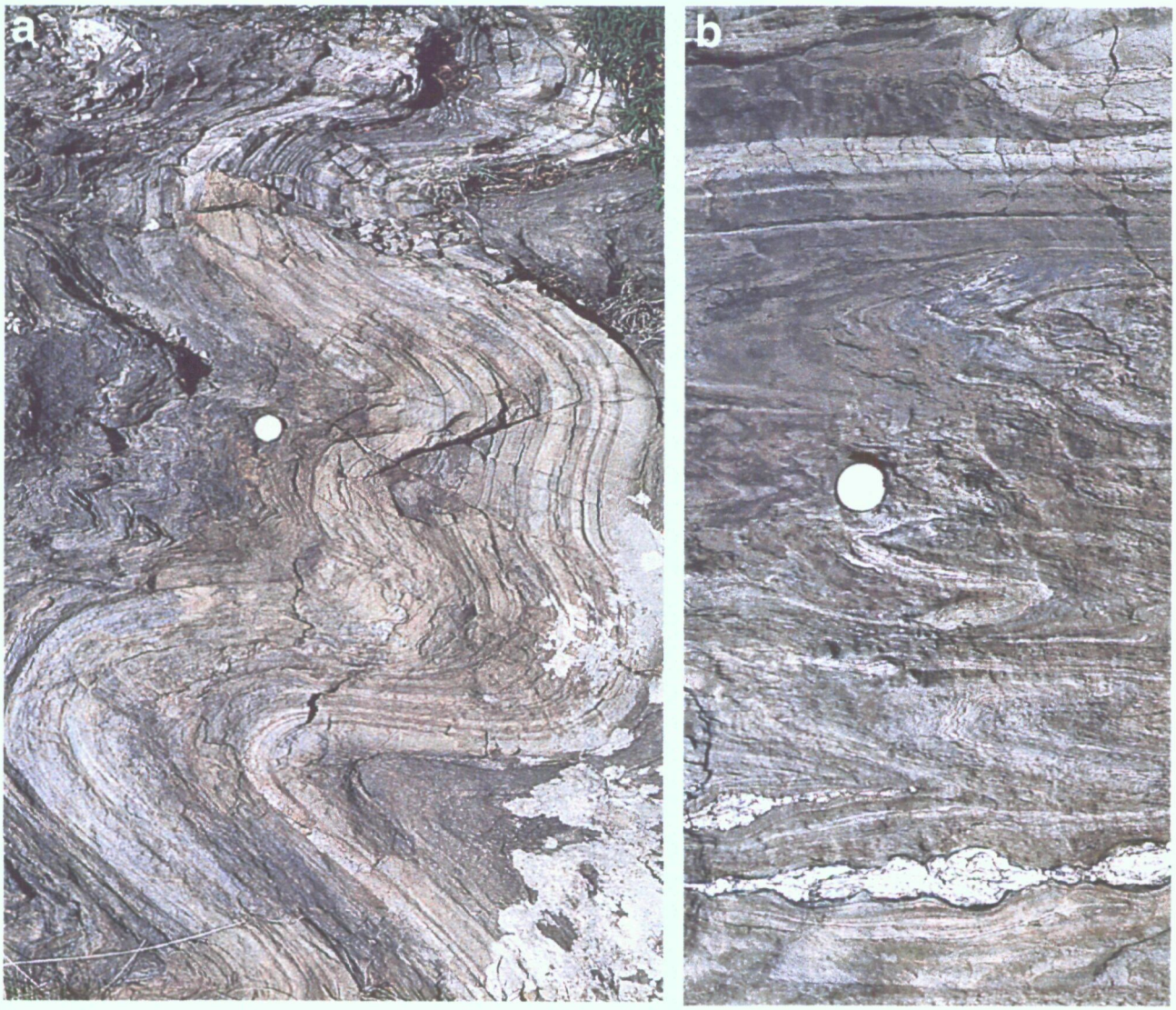

Fig. 55. Field photographs of late folds. (a): F_3 folds affecting bedding-parallel S1 foliation, Rabassers de Baix. (b): F_3 tight folds and transposition foliation in a zone of D_3 intense deformation. Pegmatite veins appear boudinaged by D_3. Outcrop between Rabassers de Dalt and Puig Alt Gran.

FIG. 54: D_3 LATE STRUCTURES NE CAP DE CREUS PENINSULA

U.T.M. 522.5

U.T.M. 525

U.T.M. 4687.5

U.T.M. 4685

poles to mylonitic foliation
n=1279

mylonitic stretching lineation
n=635

F_3 fold axes and L_3 crenulation lineation
n=488

poles to axial planes of F_3 folds, S_3 axial planar foliation and crenulation cleavage
n=535

punta dels Farallons
volt Andrau
punta del Moll
cala Sardina
cala Prona
cala Serena
cala de sa Tuna
punta dels Tres Frares
cap de Ravaner
cala Ravaner
racó de s'Arenalona
canal Guillosa
illa de Portalló
es Xiulet
cala Galladera
cala Tavallera
Tudela
cala d'Aiguina
illa de Cullaró
racó de Francalis
cala Cullaró
es Conill
illa Encalladora
cala Culip
puig de Culip
sa Clavegadora
Cap de Creus
lighthouse
cova de s'Infern
cala Fredassa
cala Jugadora
puig de ses Formigues
sos Orgues
cala Roca
cala Torta
racó de Codera
badia de Guillola
es Jonquet
s'Alqueria
illa de Portlligat
badia de Portlligat
CADAQUÉS
puig de cala Sardina
puig d'en Melus
roca dels Marroquins
mas de la Birba
puig d'en Climat
mas Rabassers de Baix
mas Rabassers de Dalt
puig Alt Gran
puig des Campes Conreats
LA FANGAL
puig Alt Petit
coll de sa Fruita
puig Falcó
puig de sa Silvina
mas d'en Gomela
mas d'en Duran
puig de l'Infern
puig dels Bufadors
puig Carallot
MUNTANYA NEGRA
puig Ferrat

1 km

scale: 1:20000

- shear zones
- transition zone
- transposition bands
- axial traces of late folds and crenulation foliations

In areas of straight bedding-S_1 foliation, D_3 low strain structures are characterized by minor folds and crenulation cleavages. In the pelitic layers, a S_2 crenulation cleavage shows the effects of D_3, whereas the psammitic layers are undisturbed or show only "Z" shaped minor F_3 folds (Fig. 56).

F_3 major folds are commonly observed adjacent to (i) transposition bands in the south, and to (ii) shear zones in the central area (transition zone).

An example of the first case is given by the structures developed around metabasite outcrops to the south of Puig Alt Petit. Two major bodies of pre-Hercynian amphibolites which seem to correspond to the same intrusion have been folded with an axial planar S_3 transposition foliation (Structural Map). The adjacent metasediments display tight F_3 folds, gradually evolving into the transposition foliation.

An illustrative example of the association of folds and shear zones is shown in Fig. 57, where axial planes and crenulation cleavages are nearly parallel to the shear zones. The shear zones appear as stretched limbs of these folds, due to strain intensification along narrow bands.

In zones of local D_2 or D_{2-3} mesoscale folding, much more complex structural patterns arise from D_3 overprinting. This is the case, for instance, of the Mas de la Birba and the Coll de Sa Freita-Mas Rabassers de Dalt areas.

The Coll de Sa Freita-Mas Rabassers de Dalt area illustrates the structures resulting from superposed folding. Quartzite beds have been used as markers for the recognition of large scale fold interference structures (Fig. 58). In sub-horizontal surfaces, the main quartzite bed form two mushroom-like forms which are compatible with a superposition of F_3 folds on previous F_2 (and maybe F_{2-3}) folds. The structures observed in the adjacent metasediments confirm the presence of D_2 and later D_3 crenulation cleavages. The first D_2 folds in the quartzite, which were possible "S" shaped, were later refolded during the D_3 event. The E-W to NW-SE F_3 folds would adopt different shapes depending in which limb (short or long) of the previous folds they developed, giving place to the present mushroom shape.

Besides, in the La Birba case, F_3 folds affects an already complex previous pattern characterized by heterogeneous deformation, with domains of low and high D_2 strain (Fig. 44 in section 4.3.2 and Structural Map). A N-S vertical section across the zone (Fig. 59) also shows this complex pattern. Fold axes in this area plunge moderately to the east, so that the cross-section cuts them obliquely. A series of sub-vertical antiformal and synformal folds developed at the D_2 event. The north limb of the southernmost synform marks the entrance into the high D_2 strain domain. Both synforms involve the Sant Baldiri complex, whereas the core of the antiform in between is made of gneisses. The effect of late folds consists in tightening the previous folds, whereas an associated shear zone with normal motion produces some displacement along the north limb of the antiform. In map view, many complex structures result from superposed folding.

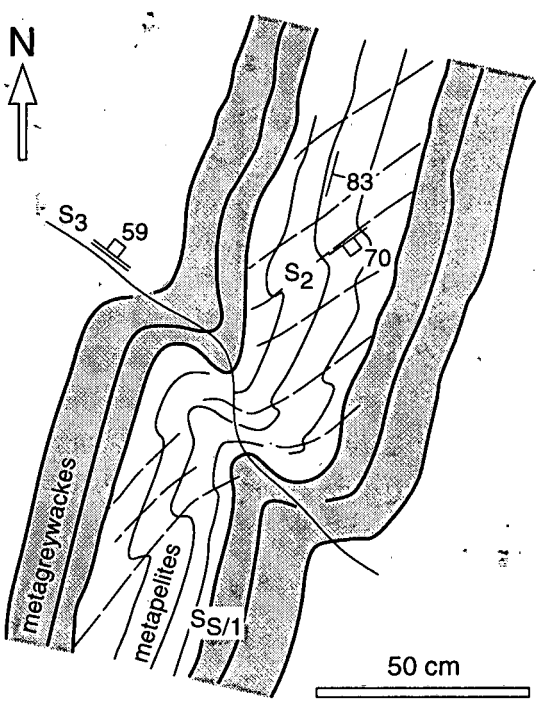

Fig. 56. Field sketch illustrating the relationships between $S_{S/1}$ S_2 and S_3 foliations in a zone of low D_2 and D_3 strain (Racó de Codera, map view).

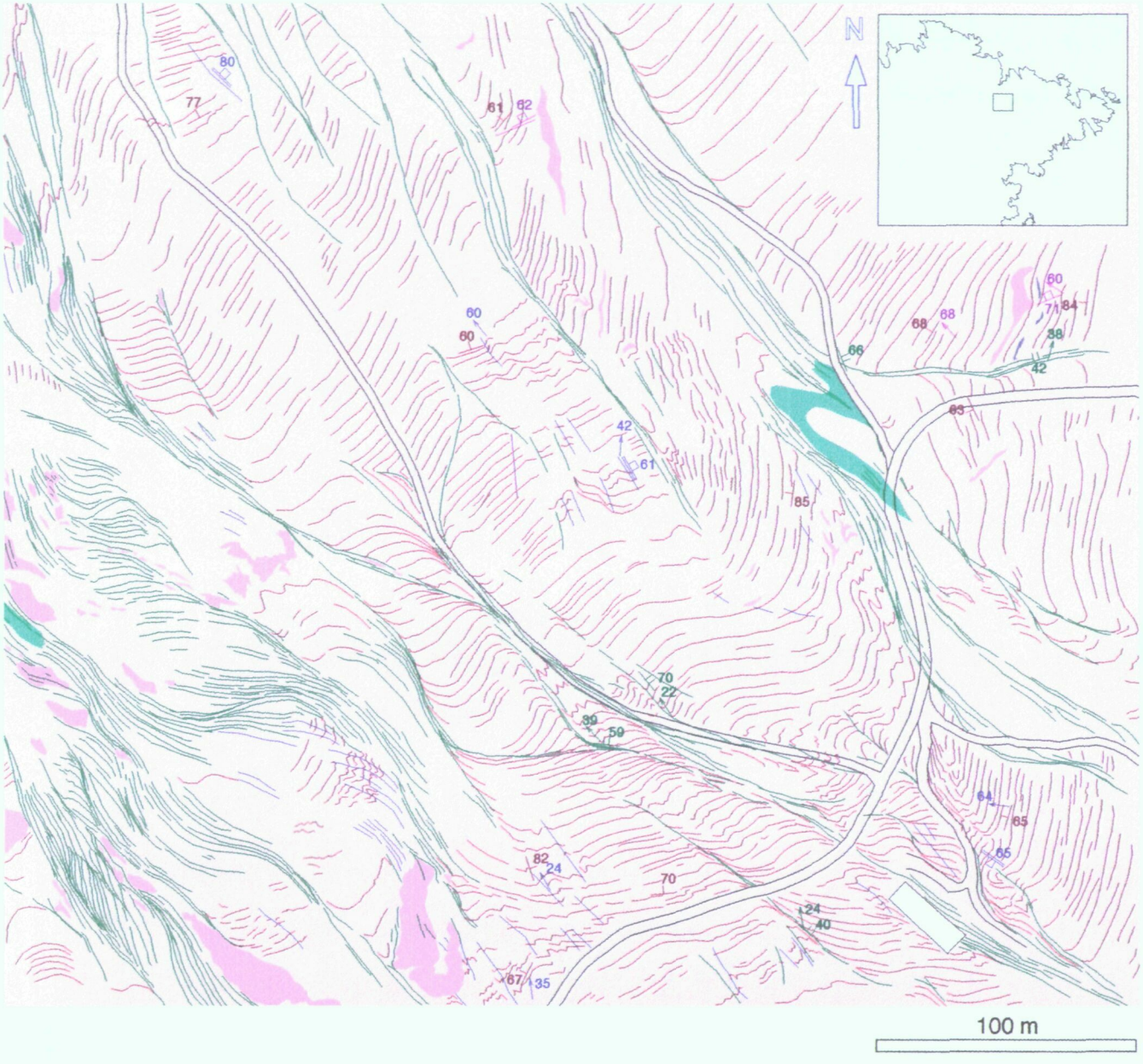

poles to mean foliations:
- S_3 mylonitic foliation
- S_3 crenulation foliation
- S_1 early foliation

same colours for mean values of foliations (the thick line is the dominant foliation)

same colours for cylindrical best fit (dashed)

○ deduced F_3 fold axis

L_3 mylonitic lineation (mean value)

L_3 crenulation lineation and F_3 fold axes (mean value)

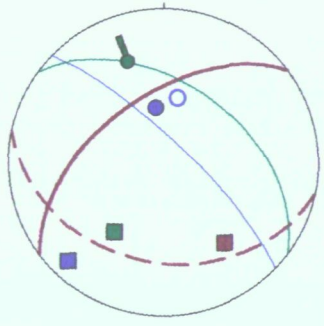

pegmatites

calc-silicate rocks (Sant Baldiri complex)

Culip type quartzites

metagreywackes and metapelites

mylonitic foliation and lineation

S_3 foliation and L_3 lineation

S_2 foliation and L_2 lineation

S_1 foliation

Fig. 57. Structural map of the Coll de ses Portes area and equal area lower hemisphere projections of mean values to main structural elements.

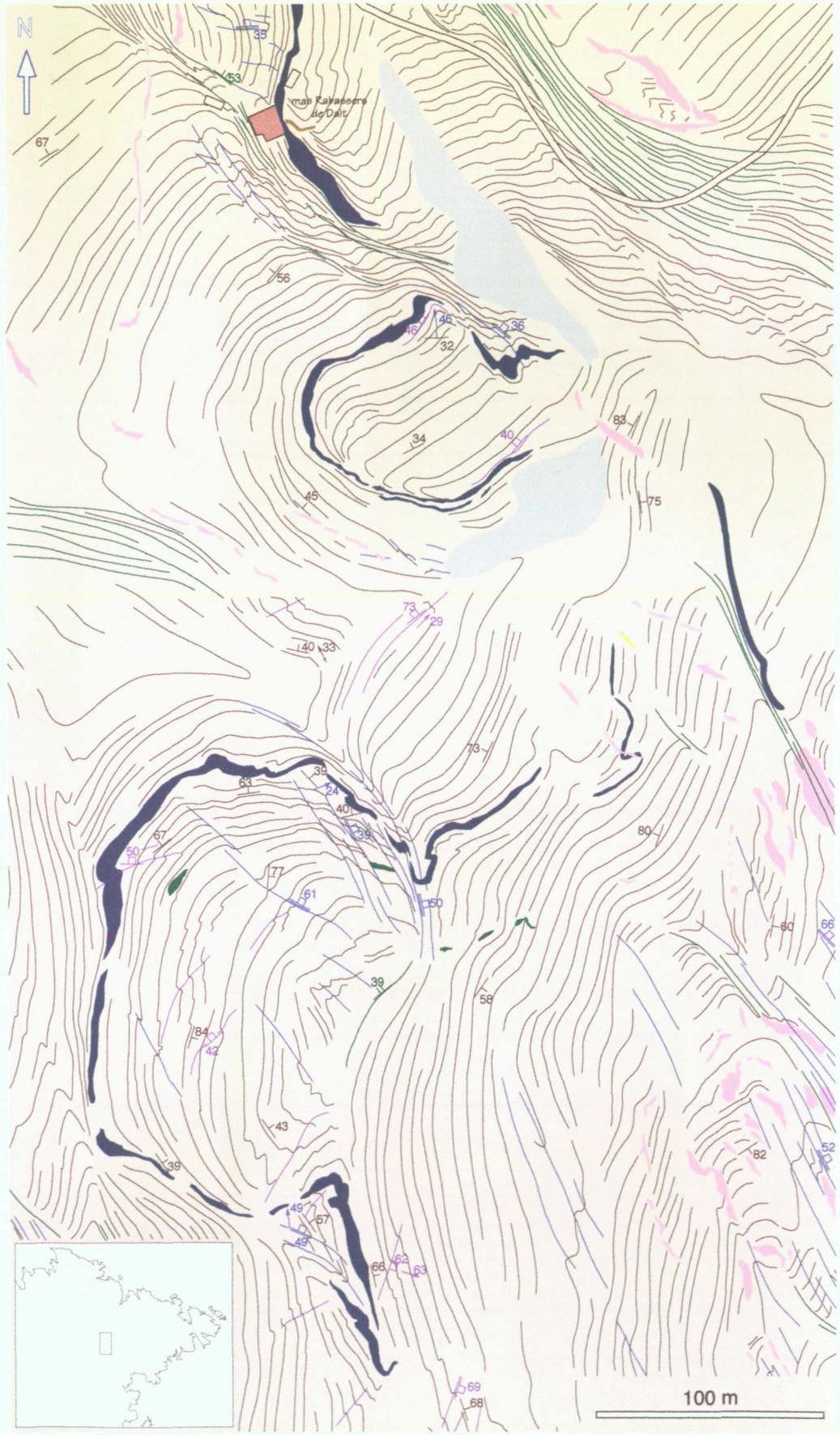

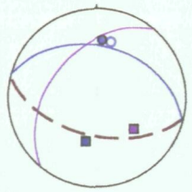

northern quartzite fold interference structure

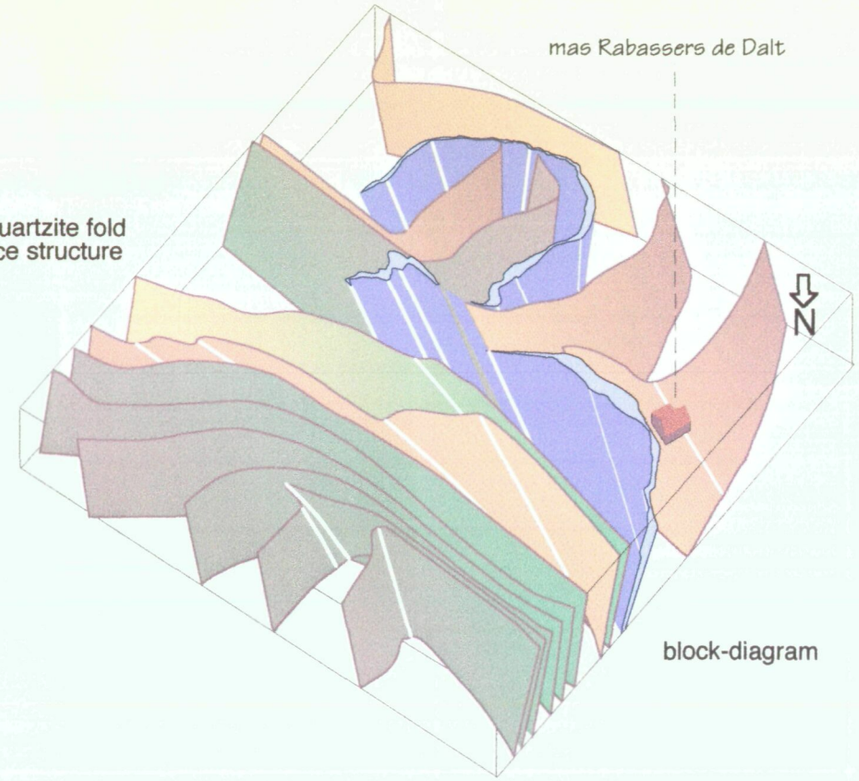

block-diagram

poles to mean foliations
- S_3 crenulation foliation
- S_2 crenulation foliation
- S_1 early foliation

same colours for mean values of foliations
(the thick line is the dominant foliation in each sub-area)
same colours for cylindrical best fits (dashed)

- deduced F_3 fold axis
- deduced F_2+F_3 fold axis
- L_2+L_3 lineations (mean value)

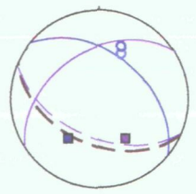

southern quartzite fold interference structure

- Quaternary deposits
- lamprophyre
- quartz veins
- pegmatites
- metabasites
- Rabassers type quartzites
- metagreywackes and metapelites

- shear zones and associated stretching lineation
- S_3 foliation and L_3 lineation
- S_2 foliation and L_2 lineation
- S_1 foliation and L_1 lineation

Fig. 58. Structural map of Coll de sa Freita - Rabassers de Dalt area and equal area lower hemisphere projections of mean values to main structural elements for two sub-areas around quartzite fold interference structures.

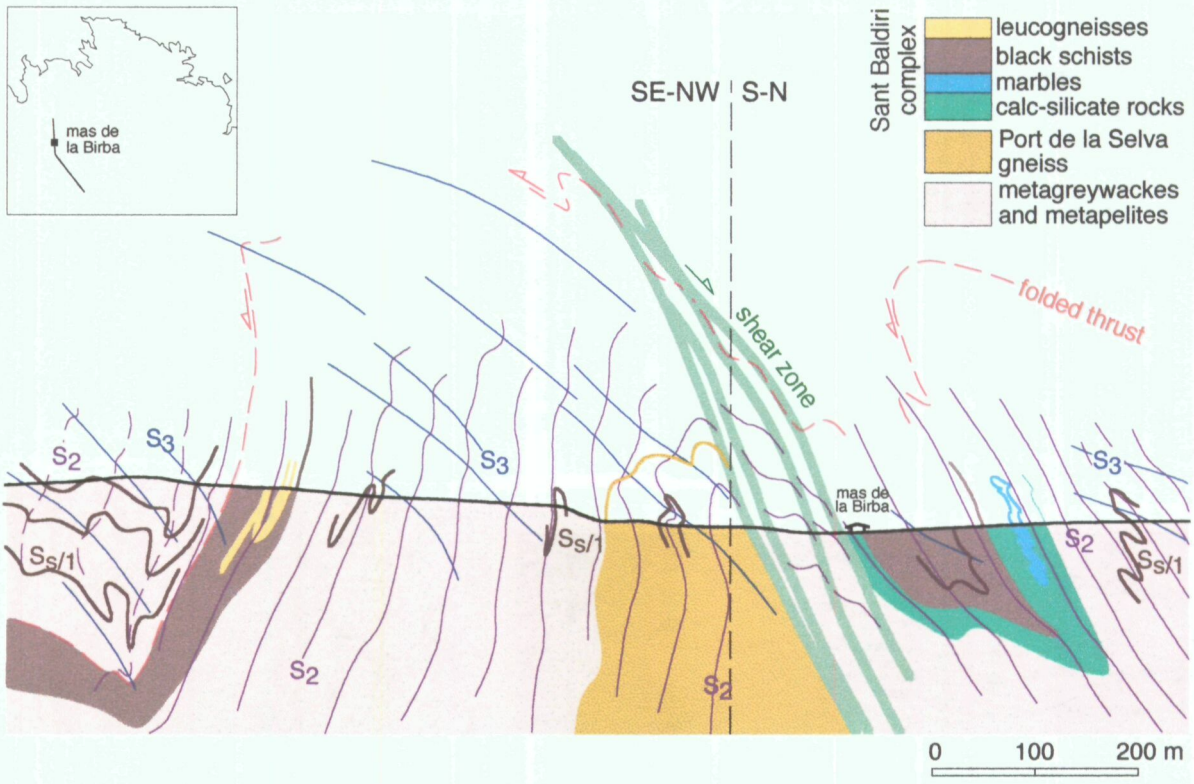

Fig. 59. Schematic cross-section across the Mas de la Birba zone.

Microstructures

Crenulations belonging to D_3 folding are associated to retrograde metamorphism at greenschists facies conditions, clearly postdating the metamorphic peak in medium and high grade rocks. Micas involved in crenulation domains are strained, often with kinkbands, and mica-fish are also common. Relic porphyroblasts are rotated (Fig. 60). Quartz forms granoblastic aggregates of new grains, preferentially located in the microlithons. Other minerals like feldspar, tourmaline and garnet remain as porphyroclasts.

The best examples of overprinting relations between S_2 and S_3 foliations are exposed in the low-medium grade millimetric alternances. As S_2 crenulations develop preferentially in the pelitic layers, later refolding also acts selectively on D_2-related cleavage domains (Fig. 61c). Many of these examples are analogous to those of selective refolding described by and Passchier & Trouw (1996, Fig. 4.36 & 4.37).

Grain size reduction is most important within bands of intense S_3 folding, where protomylonitic to mylonitic microstructures develop. In these high strained rocks, porphyroblasts tend to disappear by alteration into pinite.

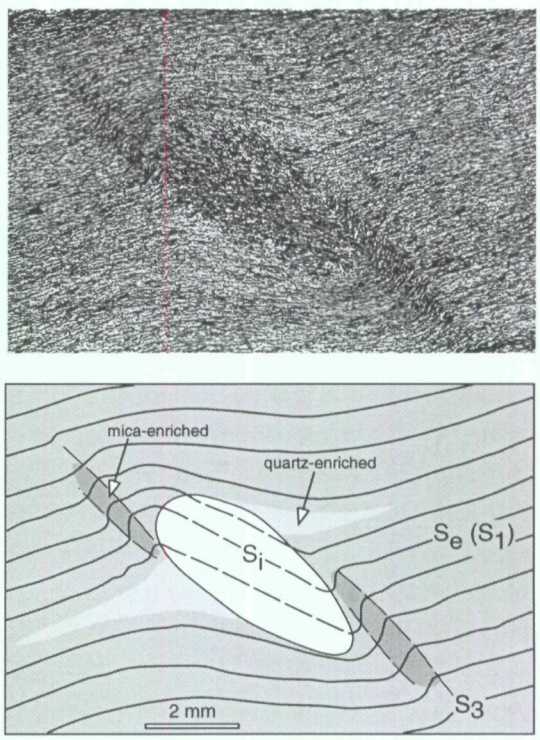

Fig. 60. Relative rotation of a porphyroblast of cordierite with respect to the S_1 foliation (about 45° clockwise). Note the related development of quartz- and mica-enriched domains and S_3 microfolds.

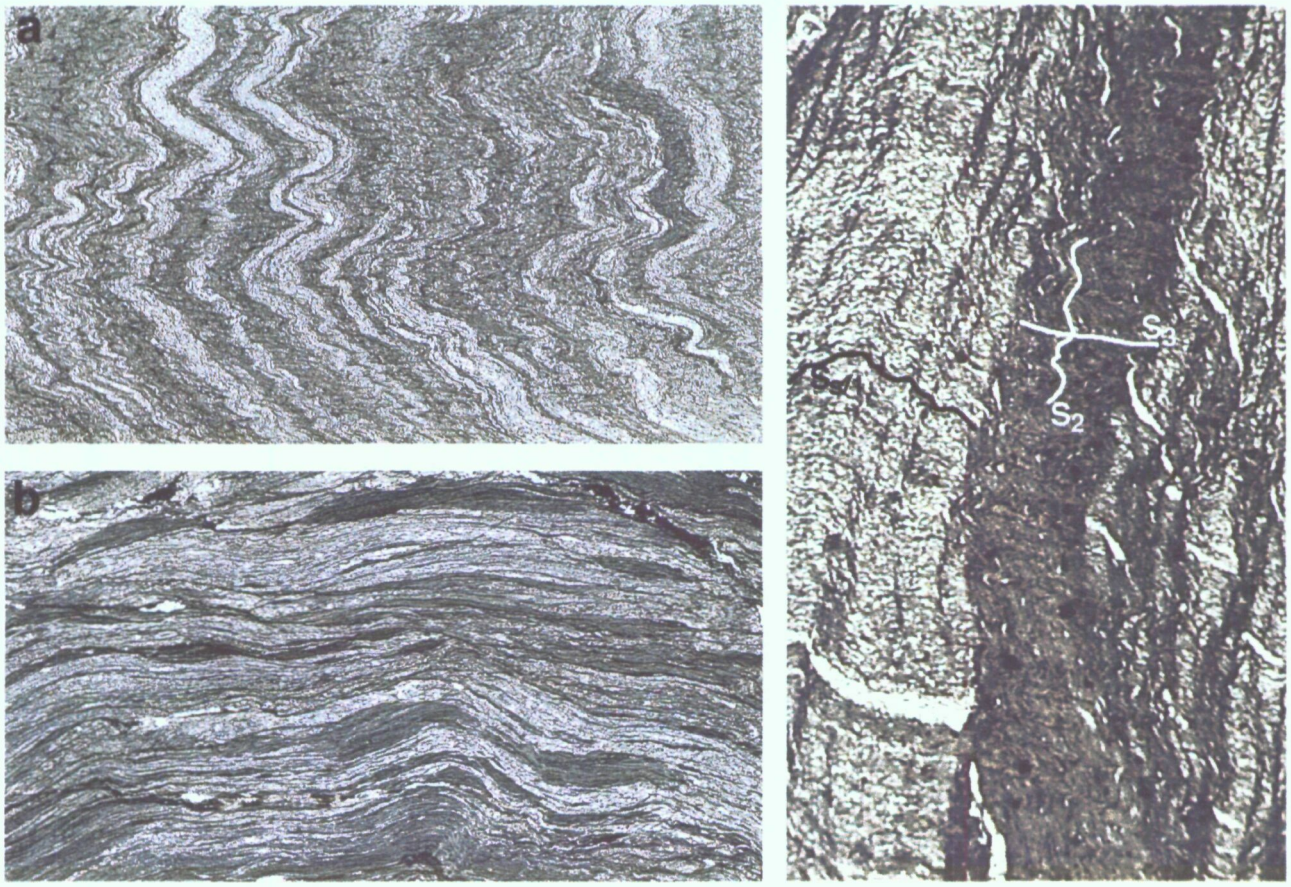

Fig. 61. Photographs of D_3 microstructures. PPL. (a): Microfolds and axial planar crenulation cleavage (width of view 3 cm). (b): Effects of intense D_3 deformation in a micaschist: chloritization and development of mica-fish wrapped by a transposition foliation. Width of view 2.4 cm. (c): Example of D_3 selective refolding of a previous D_2 tectonic banding. Width of view 5 mm.

4.5.2. SHEAR ZONES

Shear zones, also ascribed to the D_3 deformation develop as an anastomosed network, in which NE dipping shear zones and associated NNW low plunging stretching lineations dominate (Fig. 54).

These shear zones are profusely described in the literature with reference to their geometry, kinematics, microstructures, microfabrics and geotectonic significance (Carreras & Santanach 1973, Carreras et al. 1977, Carreras & García 1982, Norton 1982, García 1983, Carreras 1989). Due to the available documentation, and taking into account the aim of this work, detailed descriptions will not be made, and only a brief summary of the state of the art will be presented. The main statements concerning these structures can be summarized in the following points.

Shear zones affect mainly previously foliated rocks and thus there is a variability between shear zone geometry and kinematics. High strain achieved inside the shear zones usually exceeds values of gamma>10, and thus a complete transposition of earlier fabrics is produced (Fig. 62). Kinematic analysis reveals a prevalent dextral with minor reversal shear sense. The geometry of the shear zones reveals that they approach the simple shear model, but with a slight deviation (especially marked in low strain marginal parts). This has been interpreted as indicating that the shear zones grew from an initial buckling instability with a shortening component normal to shear direction. In this model, shear zones bear not only strain gradients across but also along the shear zone.

In addition, there is a complete transition between typical shear zones and the transposition bands related to intense D_3 folding. Such transition is evidenced in shear zones cutting obliquely across the metamorphic zonation.

Fig. 62. Cala Prona shear zone.

As mentioned before, I will not enter in the general description of the former statements. The discussion on the effects of the D_3 shear zones will be restricted to aspects specially significant for the aim of this work: the effects on the metamorphic zonation and distribution of the igneous rocks, and the effects on the previous fabrics.

Offsetting effects

The bulk effect of the late shear zones is the development of an assemblage of elongated bodies wrapped by anastomosed mylonitic bands (Structural Map), without major discontinuities. The NW-SE trending shear zones have a predominantly dextral movement, with a minor reverse component. The reverse component increases as shear zones acquire E-W trends, with dominant dip-slip reverse motion in those trending WSW-ENE (Carreras et al. 1982). However, some of the shear zones with orientations close to E-W evidence opposite movements, with normal and sinistral components. Kinematically, the E-W shear zones are the most complicate to analyse, because they bear complex internal fabrics (shear bands, intramylonitic folds and sets of oblique stretching lineations) that reveals a polykinematic history, in which dip-slip motions predate the sub-horizontal ones.

Broadly speaking, the relation between the width and the displacement associated to a mylonite band is, at most, of two orders of magnitude. Centimetric bands show displacements of meters, and metric bands show deca- or hectometric displacements. It is inferred that shear zones neither constitute major regional discontinuities, nor juxtapose lithological units with different metamorphic and structural histories, as indicated , for instance, by the quartzite layers. This bedding-markers can be traced from low to high D_2 and D_{2-3} strain domains, as well as they are folded and sheared in domains of D_3 folds and shear zones, but they are continuous from south to north across the study area.

The largest NW-SE trending shear zones in the area produce dextral offsets of about 800 m to 1 Km. This is the case, for instance, of the shear zone between Cala d'Agulles i Cala Bona and the Cala Serena shear zone (Fig. 54 and Structural Map).

Dip-slip movements associated to the E-W trending shear zones are more difficult to estimate, although must be of similar magnitude. A complex mylonite band between Cala Ravaner and Rocal dels Marroquins (Fig. 11, Fig. 63) brings in contact the cordierite-andalusite and the sillimanite-muscovite zones. Assuming that the isogrades at this domain dip steeply to the north, minor reverse displacement is required.

The Punta dels Farallons area represents an illustrative example of how shear zones can constrain the final geological and structural patterns (Fig. 64). In this area, the combined effect of the predominantly dextral-reverse movements with the previous sinistral-normal movement along the shear zones is responsible for the configuration of the migmatite complex, which is now found in separate outcrops, surrounded by non migmatitic schists.

Effects on the previous fabrics

Two main processes are involved in mylonitization. One is the partial retrogradation of the original rock-forming mineralogy into greenschists facies assemblages, and the other is the microstructural change, which led to a drastic grain size reduction (Carreras et al. 1975, 1977). These mineralogical and microstructural transformations have already been described in section 3,2.4.

As a consequence of high ductile strain, all previous fabrics are transposed, and the layering present in the rocks of the metasedimentary sequence rotates into parallelism with the mylonitic foliation. Other compositional heterogeneities as quartz segregation veins, pegmatites, migmatites and granitoids can also be mylonitized, being transformed into quartz- and quartzofeldspathic mylonites. However, these

original compositional heterogeneities are preserved within the new mylonitic banding.

Pegmatites and granitoids with minor internal fabrics acquire as a mylonitic penetrative foliation and are transformed into banded gneisses (Fig. 65). In the same way, mylonites derived from highly heterogeneous migmatites also display banded gneiss textures. Similar examples on the development of banded gneisses by intense deformation of heterogeneous igneous rocks have been reported by Myers (1978) and Passchier et al. (1990).

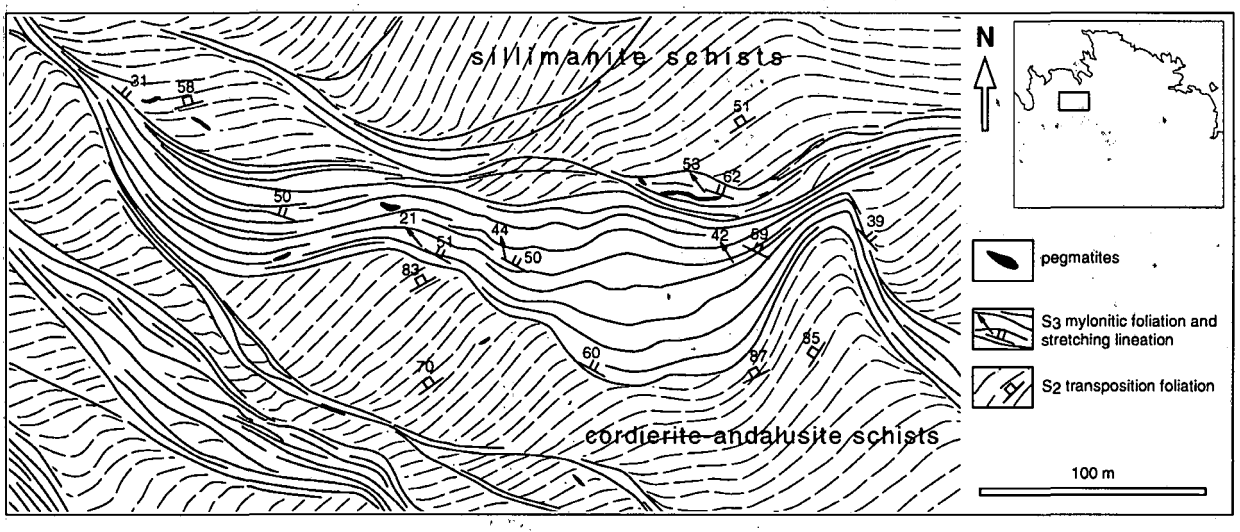

Fig. 63. Structural map of southeast Cala Ravaner area.

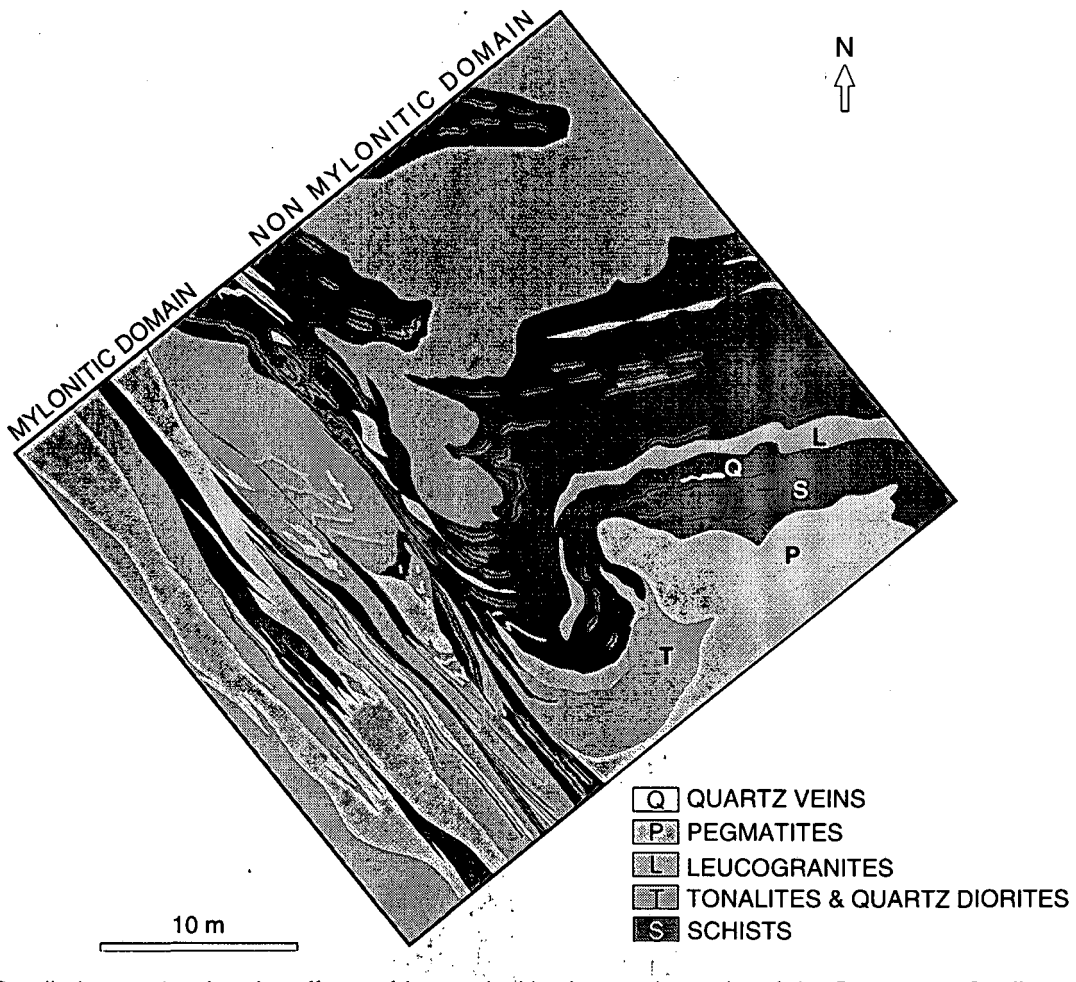

Fig. 65. Detailed map showing the effects of late mylonitization on the rocks of the Punta dels Farallons migmatite complex (after Carreras and Druguet 1994b). Location in Fig. 64.